3296 J. Med. Chem. 2010, 53, 3296–3304
DOI: 10.1021/jm100034x

Journal of Medicinal Chemistry Article

Identification of Phenylsulfone-Substituted Quinoxaline (WYE-672) as a Tissue Selective Liver X-receptor (LXR) Agonist

Baihua Hu,*,† Rayomand J. Unwalla, Igor Goljer,† James W. Jetter,† Elaine M. Quinet,‡ Thomas J. Berrodin,‡ Michael D. Basso,‡ Irene B. Feingold,§ Annika Goos Nilsson,∥ Anna Wilhelmsson,∥ Mark J. Evans,‡ and Jay E. Wrobel†

†*Chemical Sciences, Wyeth Pharmaceuticals, 500 Arcola Road, Collegeville, Pennsylvania 19426,* ‡*Cardiovascular and Metabolic Diseases, Wyeth Pharmaceuticals, Collegeville, Pennsylvania 19426,* §*Biotransformation and Disposition, Wyeth Pharmaceuticals, Collegeville, Pennsylvania 19426, and* ∥*Karo Bio AB, Huddinge, Sweden*

Received January 11, 2010

A series of phenyl sulfone substituted quinoxaline were prepared and the lead compound **13** (WYE-672) was shown to be a tissue selective LXR Agonist. Compound **13** demonstrated partial agonism for LXRβ in kidney HEK-293 cells but did not activate Gal4 LXRβ fusion proteins in huh-7 liver cells. Although **13** showed potent binding affinity to LXRβ (IC_{50} = 53 nM), it had little binding affinity for LXRα (IC_{50} > 1.0 μM) and did not recruit any coactivator/corepressor peptides in the LXRα multiplex assay. However, compound **13** showed good agonism in THP-1 cells with respect to increasing ABCA1 gene expression and good potency on cholesterol efflux in THP-1 foam cells. In an eight-week lesion study in LDLR −/− mice, compound **13** showed reduction of aortic arch lesion progression and no plasma or hepatic triglyceride increase. These results suggest quinoxaline **13** may have an improved biological profile for potential use as a therapeutic agent.

Introduction

Liver X receptors, LXRα[a] (expressed in adipose, intestine, liver, kidney, and macrophages) and LXRβ (expressed ubiquitously), are members of the nuclear hormone receptor super family and are involved in the regulation of cholesterol and lipid metabolism.[1−4] They are ligand-activated transcription factors and bind to DNA as obligate heterodimers with retinoid X receptors (RXR). Activation of LXRs (1) promotes transactivation of ATP-binding cassettes (ABCA1, ABCAG1) and apoE in macrophages, (2) prevents cholesterol accumulation as intracellular lipid droplets, (3) promotes cholesterol efflux from macrophages-derived foam cells of established lesions, (4) enhances reverse cholesterol transport (RCT) process, (5) reduces inflammation in lesion sites, and (6) reduces cholesterol absorption in the gut. For instance, treatment with known LXR modulators such as **1a** (TO901317),[5] **1b** (GW3965),[6,7] and **2** (WAY-254011)[8,9] (Figure 1) retard the advancement of atherosclerotic processes in mouse models of atherosclerosis. Thus, an LXR agonist may offer potential benefits on lipid metabolism, glucose metabolism, and vascular inflammation, thereby reducing the risk of cardiovascular disease. However, these synthetic LXR agonists also induce hypertriglyceridemia in the liver, mainly through the upregulation of genes in fatty acid biosynthesis, including sterol regulatory binding element protein 1c (SREBP-1c) and fatty acid synthase (FAS). Several strategies[2,3] have been proposed for improving the therapeutic index of LXR agonists including partial agonists, LXRβ subtype selective agonists, and gene or tissue specific agonists. The first hypothesis is based on the premise that the partial agonists bind to and activate the LXR receptors but elicit a smaller triglyceride (TG) response than a full LXR agonist. WAY-252623 (**3**), the first LXR agonist clinical candidate, possessed potent LXR binding affinity but was a weak partial agonist in Gal4 transactivation assays, particularly on LXRα relative to pan agonist **1a**.[10] Compound **3** demonstrated efficacy for reduction of aortic arch lesion progression in a LDLR −/− atherosclerosis mice model. In addition, this compound upregulated LXR target gene expression (ABCA1 and ABCG1) in the duodenum of hamsters[10] and in whole blood of cynomolgus monkeys and humans.[11] Compound **3** did not have significant effect on plasma or hepatic lipids in LDLR −/− mice[11b] or hamsters.[10] In cynomolgus monkeys, the compound had no effect on plasma lipids but did increase hepatic lipids dramatically at the highest dose tested.[11b] Although this hepatic TG increase may not be due directly to LXR induced lipogenic gene regulation,[11b] we felt it was necessary to further improve our compound profile with respect to these lipid effects and therefore strove to achieve greater selectivity over LXRα. Efforts to minimize side effects through selective targeting of the LXR β-isoform are based on the premise that LXRα is the predominant subtype expressed in the liver and that activation of LXRα may be responsible for the observed increase in hepatic lipogenesis. Recent studies provide confirmation that selective LXRβ activation reversed atherosclerosis and cellular cholesterol overload in mice lacking LXRα and ApoE.[12] Unfortunately, there

*To whom correspondence should be addressed. Phone: 609-619-3517. E-mail: bhu519@aol.com.

[a] Abbreviations: LXR, liver X receptor; ABCA1/G1/G5/G8, adenosine triphosphate binding cassette, A1/G1/G5/G8; HepG2, human hepatocellular liver carcinoma cell line; THP-1, Human acute monocytic leukemia cell line; LDLR−/−, low density lipoprotein receptor knockout; TG, triglycerides; RXR, retinoic acid X receptor; RCT, reverse cholesterol transport; SREBP-1c, sterol regulatory binding element 1c; FAS, fatty acid synthase; LBD, ligand binding domain; PPARs (α, γ, or δ), Peroxisome proliferator-activated receptor α, γ, or δ; FXR, farnesoid X receptor; PXR, pregnane X receptor; TR, thyroid receptor; NADPH, the reduced form of nicotinamide adenine dinucleotide phosphate; GSH, glutathione; UDPGA, uridine 5′-diphospho-glucuronic acid; HEK 293, human embryonic kidney 293 cells.

 Published on Web 03/30/2010

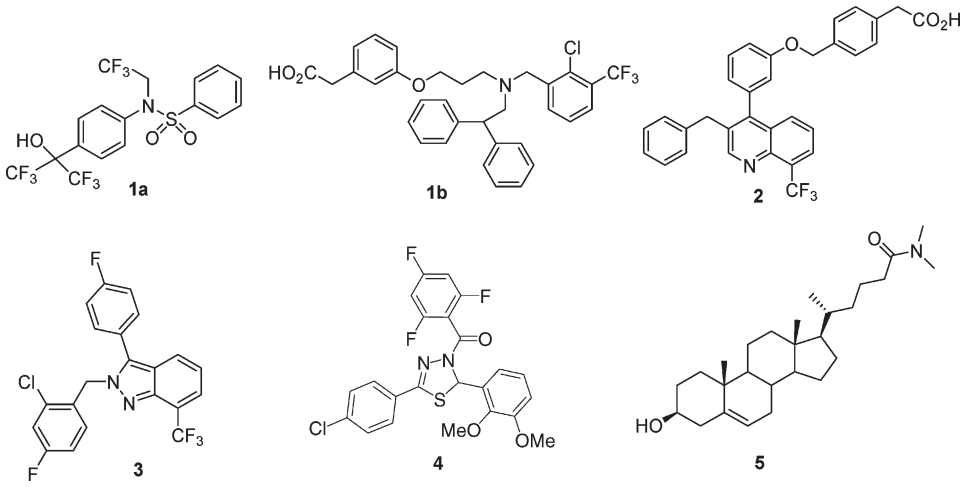

Figure 1. Known LXR agonists.

Scheme 1[a]

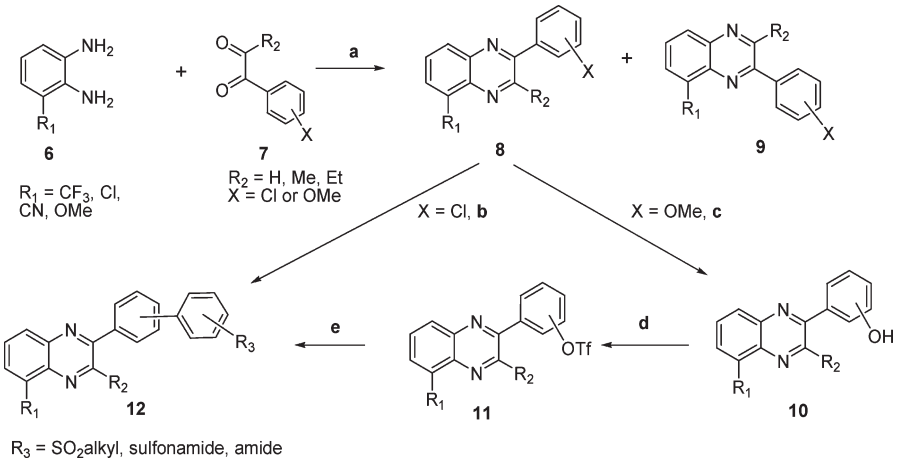

[a] Reaction conditions: (a) EtOH or MeOH, RT; (b) $Pd(OAc)_2$, 2-dicyclohexylphosphino-2′,6′-dimethoxybiphenyl, *n*-BuOH; (c) HBr or BBr_3; (d) *N*-phenylbis(trifluoromethanesulfonamide), KO^{t}Bu, THF, 0°C to RT; (e) $ArB(OH)_2$, $Pd(PPh_3)_4$, K_3PO_4, dioxane, reflux.

are only minor structural differences in the ligand binding domains (LBD) of LXRα and LXRβ that can be exploited to obtain LXRβ-selective ligands. The two LXR isoforms α/β share a high sequence identity (78%) and residue differences are located far away from the ligand binding pocket.[13] This high similarity in the binding pocket of the two LXR isoforms constitutes a serious obstacle to the development of highly β-selective ligands. Nevertheless, a modest level of LXRβ selectivity in a small molecule has been achieved. *N*-Acylthiadiazoline **4** with preferential affinity for LXRβ in scintillation proximity assays (SPA) has been reported.[14] However, **4** was found to be highly protein-bound and no in vivo efficacy (ABCA1 or SREBP1C induction) was observed in mice. *N*,*N*-Dimethyl-3β-hydroxycholenamide (**5**), a synthetic oxysterol, is a gene-selective LXR modulator that mediates potent transcriptional activation of ABCA1 gene expression while exhibiting minimal effects on SREBP-1c both in vitro and in vivo in mice (dosed by IP injection only).[15] Compound **5** stimulated cholesterol transport through the upregulation of LXR target genes in liver, small intestine, and peritoneal macrophages. However, **5** exhibited only limited activity for increasing hepatic SREBP-1c mRNA without altering the plasma TG. Unfortunately, **5** had poor pharmacokinetic properties, which may limit **5** for potential use as a therapeutic agent. In this report, we describe the identification and SAR of a novel series of phenyl sulfone substituted quinoxalines leading up to the discovery of **13** (WYE-672) as an orally active and tissue selective LXR agonist which reduced atherosclerotic lesion size in LDLR −/− mice without increasing plasma or hepatic TG levels.

Chemistry

It has been demonstrated by Wyeth that heterocycle scaffolds such as quinoline,[8] indazole,[10] cinnoline,[16] benzimidazole,[17] and quinazoline[18] can be utilized to afford potent LXR agonists. In an attempt to enlarge the chemical diversity of LXR ligands, we prepared a series of quinoxalines derivatives as shown in Scheme 1. Condensation of 1,2-diaminobenzenes **6** with 1,2-dioxoalkane **7** gave a mixture of position isomers which were separated into **8** and **9**. The regiochemistry of **8** and **9** was assigned by $^1H-^{15}N$-gHMBC NMR experiments. Reaction of **8** (X = Cl) with phenylboronic acids under Suzuki conditions provided **12**. Alternatively, deprotection of the methoxy group of **8** (X = OMe) by treatment with HBr or BBr_3 led to phenol **10**. Phenol **10** was converted to triflate **11** by using *N*-phenylbis(trifluoromethanesulfonamide) in the presence of triethylamine. The resulting triflate **11** was coupled to aryl boronic acids to give the biaryl derivatives **12**.

Table 1. LXR Binding Affinities of Quinoxalines[a]

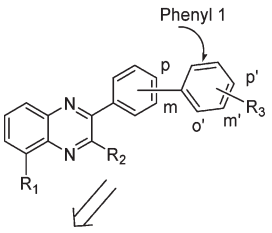

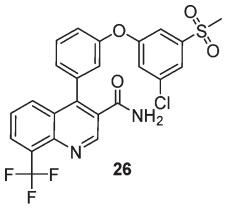

compd	R_1	R_2	position	R_3	LXRβ	LXRα
1a					0.009	0.013
13	8-CF_3	Me	p, m′	SO_2Me	0.053	> 1
14	8-CF_3	Me	p, p′	SO_2Me	> 1	> 1
15	8-CF_3	Me	p, o′	SO_2Me	> 1	> 1
16	8-CF_3	Me	m, m′	SO_2Me	> 1	> 1
17	8-CF_3	Me	m, p′	SO_2Me	> 1	> 1
18	8-CF_3	Me	p, m′	SO_2Et	0.132	> 1
19	8-CF_3	Me	p, m′	SO_2NHMe	0.081	> 1
20	8-CF_3	Me	p, m′	CONHMe	> 1	> 1
21	8-CF_3	Et	p, m′	SO_2Me	0.018	0.165
22	8-CF_3	H	p, m′	SO_2Me	> 1	> 1
23	8-Cl	Me	p, m′	SO_2Me	0.034	0.734
24	8-CN	Me	p, m′	SO_2Me	0.299	> 1
25	8-OMe	Me	p, m′	SO_2Me	0.395	> 1
26					0.061	1.77

[a] IC_{50} in μM. The highest concentration tested was 10 μM. Results are given as the mean of at least two independent experiments. The standard deviations for these assays were typically ±30% of the mean or less.

Results and Discussion

The LXR binding affinities of newly synthesized compounds were evaluated (Table 1) using recombinant human LXRα or LXRβ ligand binding domains (LBDs) with [^{3}H]**1a** as a tracer. Our first attempt with the quinoxaline scaffold (compound **13**) showed good LXRβ binding affinity (IC_{50} value of 53 nM) but poor potency (IC_{50} value of > 1 μM) for LXRα. SAR studies on this scaffold revealed that the meta orientation (position m′) for the methyl sulfone group (**13**) is preferred. The corresponding para (**14**, position p′) or ortho (**15**, position o′) analogues were considerably less potent. The projection of the phenyl 1 group is also critical for the activity as is evident by **16** and **17**, the meta-substituted (position m) isomers, which had LXRβ binding IC_{50} values of greater than 1 μM. Compared to **13**, the ethyl sulfone **18** (LXRβ IC_{50} = 132 nM) and methyl sulfonamide **19** (LXRβ IC_{50} = 81 nM) were slightly weaker binders. Amides were previously demonstrated by Wyeth as good replacements for the methyl sulfone group.[19] However, a few amides were prepared in the series and none of them showed appreciable LXR binding affinity, as exemplified by **20**. The group on quinoxaline C-2 also had big impact on the LXR binding affinity: the 2-ethyl analogue **21** is a potent LXRβ binder (IC_{50} = 18 nM), while the 2-H analogue **22** had poor binding affinity (LXRβ binding IC_{50} > 1 μM). Several small replacements[9] (compounds **23**−**25**) for the C-8 trifluoromethyl substituent were evaluated, and the chlorine once again proved to be a good replacement for the C-8 trifluoromethyl group because the 8-chloro quinoxaline **23** was a slightly more potent (IC_{50} = 34 nM) LXRβ binder than **13**.

To understand the observed SAR for the quinoxaline series, we docked[20] **13** into a previously solved in-house X-ray structure of hLXRβ complexed with compound **2**. Figure 2 shows the docked structure of **13** overlaid with the X-ray bound pose of compound **2**. Ligand recognition is achieved by 8-CF_3 group making hydrogen bond interaction with His435

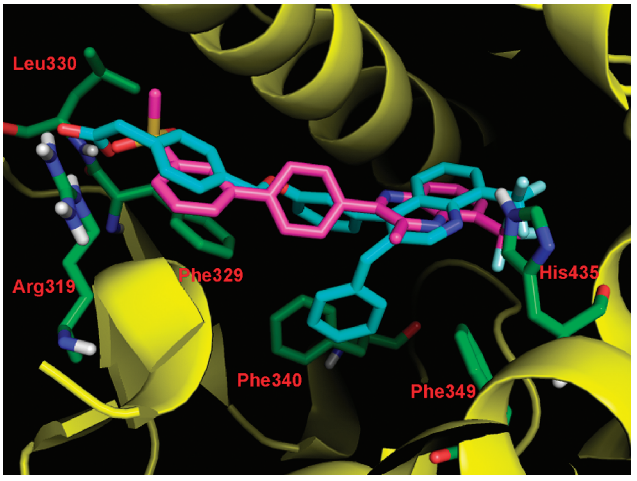

Figure 2. Docked structure of compound **13** (magenta) overlaid with the hLXRβ/**2** (cyan) X-ray complex structure Only important residues and helices are shown from the binding site.

residue, while at the distal end the sulfone oxygen made critical interaction with the backbone NH group of Leu330. There are interesting differences between the two structures with regard to the position of the core quinoline/quinoxaline rings and in the ability of these ligands to orient the critical acid/methyl sulfone groups toward the solvent exposed pocket. The N-1 atom of **13** is shifted further away from the His435 residue as the ligand tries to orient the 2-methyl group in the hydrophobic pocket occupied by the N-3 benzyl group of **2** and the C3 phenyl group of **13** has a different projection than that observed for the C4 phenyl group in the X-ray bound orientation of compound **2**. In spite of the differences in the trajectory of these phenyl groups, the terminal acid group of **2** and the methyl sulfone group of **13** are in similar position to make the critical interaction with the Leu330 NH backbone. This is a direct result of the phenyl group being able to twist out of the plane and thereby allowing the longer but flexible benzyloxy linker to orient the phenyl acetic acid group of **2** and place it in a similar position as the phenyl methyl sulfone. The small, i.e., 3-fold increase in LXRβ binding potency for compound **21** when compared to **13** is a result of the 2-ethyl group being oriented toward a hydrophobic pocket surrounded by the Phe340 and Phe349 residues and in a region where the larger 3-benzyl group of compound **2** was observed in the X-ray structure. Although the immediate residues surrounding this pocket are not different between LXRα and LXRβ, the small drop in LXRβ selectivity observed for compound **21**, i.e., ∼9-fold may due to the result of residue differences within the second shell of this region.[21]

The potent LXRβ binders from Table 1 (Compound **13**, **19**, **21**, and **23**) were further profiled in the Gal4 transactivation assays in huh-7 liver cells and cellular assays (ABCA1 expression in THP-1 cells, lipid accumulation in HepG2 liver cells, Table 2).[8] Literature compound **1a** is a potent full agonist for LXRα and LXRβ in the transactivation assays and showed little differentiation between ABCA1 gene activation versus cellular TG synthesis. In contrast, **13** showed a very favorable profile as an LXR modulator: it increased ABCA1 gene expression in THP-1 cells with a nearly full efficacy (79%) and it had very low efficacy (7%) for lipid accumulation. Compound **13** was tested in the Gal4 transactivation assays and was inactive (efficacy 1%) against LXRα. Surprisingly, the compound also showed basically no transactivation activity

Table 2. Cellular Activity of Selected Compounds[a]

compd	Gal4 LXRβ[b]	Gal4 LXRα[b]	ABCA1[c]	lipid accum[d]
1a	0.17 (100%)	0.14 (100%)	0.044 (100%)	0.14 (100%)
13	>1 (3.1%)	>1 (1%)	1.09 (79%)	(7%)
19	(2%)	(1%)	1.47 (55%)	(6%)
21	2.02 (70%)	3.59 (13)	0.90 (65%)	0.35 (32%)
23	0.86 (5%)	(1%)	0.29 (50%)	0.38 (18%)
26	1.70 (84%)	5.10 (36%)	1.89 (87%)	3.18 (74%)

[a] EC_{50} in μM (%eff). The highest concentration tested was 10 μM. Results are given as the mean of at least two independent experiments. The standard deviations for these assays were typically ±50% of the mean or less. [b] The % of efficacy is relative to **1a** in huh7-cell. [c] The % of efficacy is relative to **1a** in differentiated THP-1 cells. [d] The % of efficacy is relative to **1a** in HepG2 cells.

Table 3. Functional Activity in huh-7 and HEK-293 Cells[a]

	huh-7		HEK-293	
compd	LXRβ	LXRα	LXRβ	LXRα
1a	0.17 (100%)	0.14 (100%)	0.019 (100%)	0.053 (100%)
13	>1 (3.1%)	>1 (1%)	0.58 (45%)	1.7 (7%)
26	1.70 (84%)	5.10 (36%)	0.46 (48%)	10.9 (80%)

[a] EC_{50} in μM (%eff). The highest concentration tested was 10 μM. Results are given as the mean of at least two independent experiments. The standard deviations for these assays were typically ±50% of the mean or less. The % of efficacy is relative to **1a**.

(efficacy 3.1%) against LXRβ (vide infra). As expected, more potent LXRβ binders **21** and **23** showed a more potent cellular activity (Gal4, ABCA1, and lipid accumulation) over **13** while the weaker binder (**19**) showed weaker cellular activity.

We next focused on a preliminary investigation of a possible explanation why **13** had good activity in the THP-1 cells but poor activity in the huh-7 liver cells. Thus we compared **26**[21] to **13** because it had a similar binding profile (LXRβ IC_{50} = 61 nM, LXRα IC_{50} = 1.77 μM) and showed similar activity in the THP-1 cells (ABCA1 EC_{50} 1.89 μM, 87% efficacy). However, **26** was quite efficacious in the huh-7 transactivation assay (Gal4 LXRβ EC_{50} 1.7 μM, 84% efficacy). We initially suspected that the activity discrepancy between **13** and **26** might be due to the difference between the compound's stability, solubility, and/or cell permeability. However, no apparent difference in solubility, stability (mouse liver microsomes), and cell uptake in the huh-7 cells was observed[22] for the two compounds. When compound **13** was incubated with mouse and human liver microsomes (2 mg/mL) fortified with cytosol (2 mg/mL), NADPH (regenerating system), GSH (2 mM), and UDPGA (4 mM) at 37 °C for 60 min and 100% of parent compound remained, which suggested that the unique profile of **13** was not due to its metabolism. Interestingly, when compound **13** was tested against a 293 kidney-derived cell line (HEK-293)[23] based Gal4β transactivation assay, it showed reasonable activity (EC_{50} 0.58 μM, 45% efficacy, Table 3). As may be anticipated based on its poor LXRα binding potency, **13** did not activate the Gal4 LXRα fusion protein (7% efficacy) in the HEK-293 cells. In contrast, **26** and **1a** showed similar transactivation potencies and efficacies between the huh-7 liver cell line and the HEK-293 kidney cell line. Thus, **13** appears to be a tissue selective (kidney and macrophage versus liver cell) LXR ligand that dissociates the desired ABCA1 gene activation from the unwanted lipid accumulation.

Recent evidence supports the hypothesis that the lipogenic effects of LXR ligands are primarily LXRα mediated.[2,3,12] Compound **13** had little binding affinity against LXRα receptor, which may confer the observed low lipogenic effects associated with **13**. However, LXR functional activity is the result of a complex interaction between recruitment of coactivators and release of corepressors, the character of which may not be expected simply by the in vitro binding to the LBD. To further confirm the selectivity of **13** against the LXRα isoform, a ligand induced coactivator recruitment assay[11b] for probing conformational subtleties was conducted (Figure 3). In the multiplex recruitment assay, compound **13** showed very little if any interaction with the 43 cofactor peptides (Figure 3A) for the LXRα subtype, while **26** and **3** had a comparable recruitment profile to that of **1a**, albeit reduced in magnitude. However, **13**'s LXRβ peptide recruitment profile with the same set of coactivator/repressor peptides was basically the same as **1a**, **3**, and **26** (Figure 3B). These results may indicate a unique conformation associated with **13** which are consistent with the distinct pharmacology of **13** versus **26**, **3**, and **1a**.

Compound **13** when tested for its ability to stimulate [H^3] cholesterol efflux in THP-1 foam cells induced cholesterol efflux in a concentration-dependent manner, consistent with its ability to induce ABCA1 gene expression. Notably, in this assay, compound **13** had good potency (EC_{50} value of 72 nM for **13** versus 4 nM for **1a**) and efficacy (60% relative to **1a**).

Compound **13** was screened against a panel of 23 nuclear receptors, and it did not display agonist or antagonist activity against closed related receptors such as PPARs (α, γ, δ), FXR, PXR, RXR, GR, MR, AR, PR, ER, and TR (data not shown).

After being administered at a 10 mg/kg PO dose in 2% Tween 80/0.5% methylcellulose to fasted male C57 mice, compound **13** showed reasonable oral PK parameters: it had a long half-life ($t_{1/2}$ > 20 h) and the C_{max}, $AUC_{0-\infty}$, and T_{max} were 229 ng/mL, 2439 h·ng/mL, and 4 h, respectively. An accelerated atherosclerotic lesion study was conducted in high fat/high cholesterol (1.25%)-fed LDLR−/− mice (n = 12 per group) for 8 weeks. Either 0.6 mg/kg/day or 3 mg/kg/day of **13** admixed in the feed resulted in a significant reduction in lesion burden by 20% ($p < 0.05$), and 51% ($p < 0.001$), respectively, compared to the control group. In the same experiment, the literature standard **1b** (dosed at 10 mg/kg) also significantly reduced the lesion burden by 41% (n = 12, $p < 0.001$). The average plasma concentrations of **13** were 1019 ng/mL and 10782 ng/mL for the 0.6 mg/kg and 3 mg/kg dose, respectively (at 3 h following 8 week of daily dosing in feed). The average plasma concentration of **1b** was 175 ng/mL. Neither **13** nor **1b** had a significant effect on total plasma cholesterol levels or on plasma or hepatic triglyceride levels. In addition, the effects of compound **13** on LXR responsive genes were monitored in several tissues. In the duodenum, **13** at both doses and **1b** significantly induced ABCA1, ABCG5, and ABCG8 gene expression (Figure 4). Similarly, **13** at both doses and **1b** induced ABCA1 and ABCG1 expression in mononuclear peritoneal macrophages (Figure A in the Supporting Information section). In contrast, as shown in Figure 4, in the duodenum **13** exhibited much weaker activity for SREBP1c gene expression compared to **1b**. In liver, neither compound (**13** or **1b**) induced hepatic SREBP-1c gene expression and both showed little regulation of LXR target genes. (Figure B in the Supporting Information).

Conclusion

In summary, we have described the identification of phenyl sulfone substituted quinoxaline **13** as a tissue selective LXR agonist. The tissue selectivity was observed in Gal4 transactivation assays in liver huh-7 cells versus kidney HEK-293 cells. It showed partial agonism for LXRβ in HEK-293 cells but did not activate Gal4 LXRα fusion proteins in either HEK-293

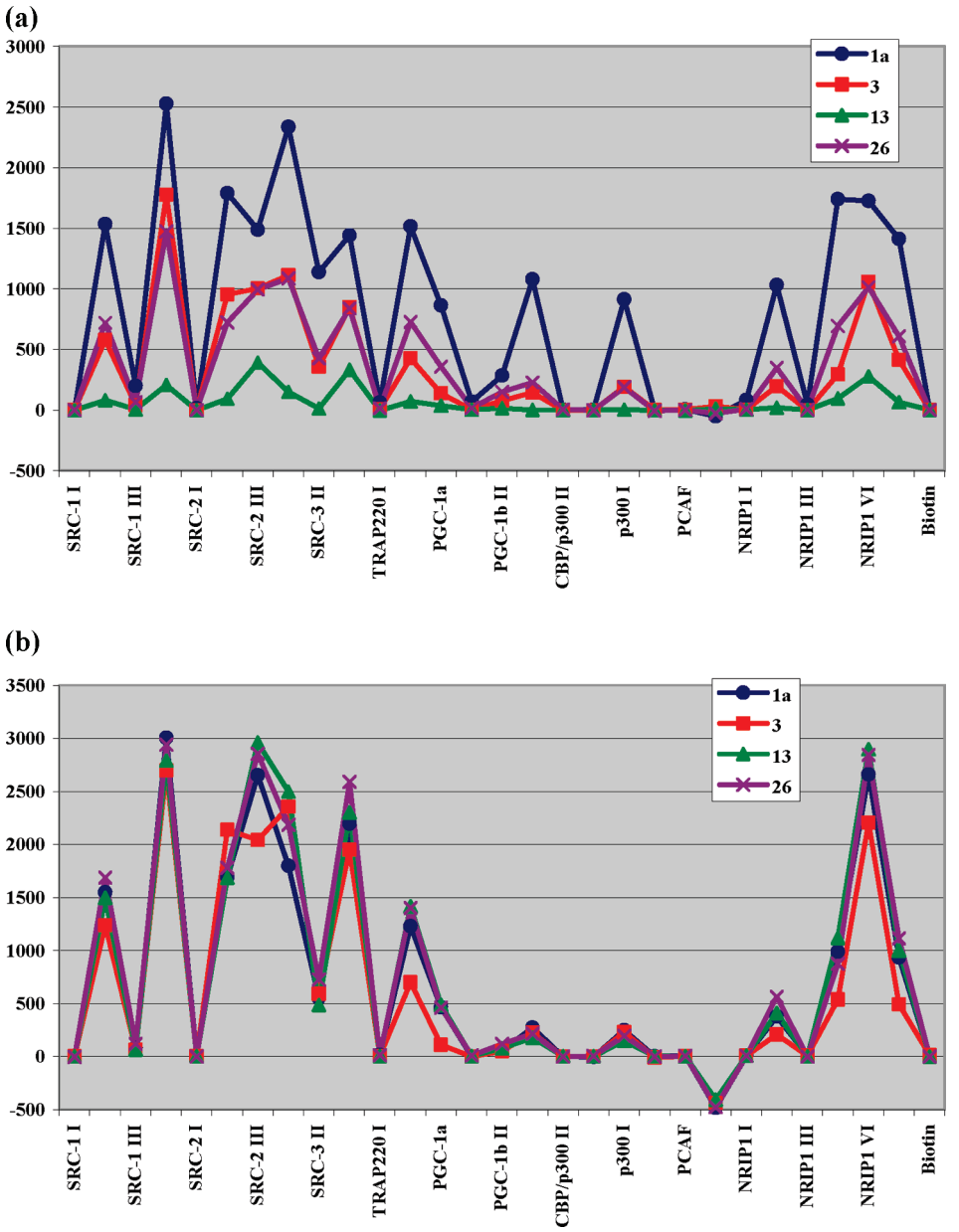

Figure 3. Effect of **13**, **1a**, **3**, and **26** on recruitment of cofactor peptides on human LXRα and LXRβ LBD proteins. The LXR multiplex assay was performed with 10 μM concentration. (a) (top) represents LXRα and (b) (bottom) for LXRβ. The mean fluorescence intensity for treatments was plotted on the *Y* axis.

cell line or huh-7 cell line. Quinoxaline **13** showed poor binding affinity to LXRα in the binding assay and did not recruit coactivator/corepressor peptides in a LXRα multiplex assay. Compound **13** showed good agonism in THP-1 cells (79% relative to **1a**) with respect to increasing ABCA1 gene expression and good potency (EC_{50} = 72 nM) on cholesterol efflux in THP-1 foam cells. In an eight-week lesion study, compound **13** showed reduction of aortic arch lesion progression and stimulation of LXR genes in the duodenum without inducing the plasma or hepatic TG levels. Therefore, **13** may be a promising agent for the treatment of atherosclerosis.

Experimental Section

General Methods. All experiments were conducted in well-ventilated fume hoods. Anhydrous solvents were purchased from Aldrich Chemical Co. (Milwaukee, WI) and used directly. Bulk solvents and chemicals were purchased from EMD and used directly. ^{1}H NMR were recorded on Varian INOVA 400 MHz, Bruker AVANCE II 400 MHz, and Bruker AVANCE II 300 MHz instruments in the indicated solvent at 20 °C. Chemical shifts (δ) are expressed in ppm downfield from tetramethylsilane (TMS). High resolution mass spectra were recorded on an Agilent 6210 TOF instrument. Positive and negative electrospray mass spectra were recorded on Waters ZQ or ZMD instruments.

The following HPLC methods were used to determine purity of intermediates and final products. All final products tested in biological assays were ≥95% pure. Method A: column, Xterra MS C18, 5 μ, 50 mm × 2.1 mm. Mobile phase: A, 10 mM ammonium formate in water (pH 3.5); B, 50:50 ACN:MeOH, for 2 min, hold 1.5 min. Sample concentration: 2.000 g/L. Temperature: room temperature. Flow rate: 0.8 mL/min. Detection: 210−370 nm. Method B: Column Xterra reverse phase C18, 3.5 μ, 150 mm × 2.1 mm. Mobile phase: A, 85/15−5/95 (ammonium formate in water, pH 3.5; B:ACN + MeOH, for 10 min, hold 4 min. Temperature: 40 °C. Flow rate: 0.8 mL/min. Detection: 210−370 nm.

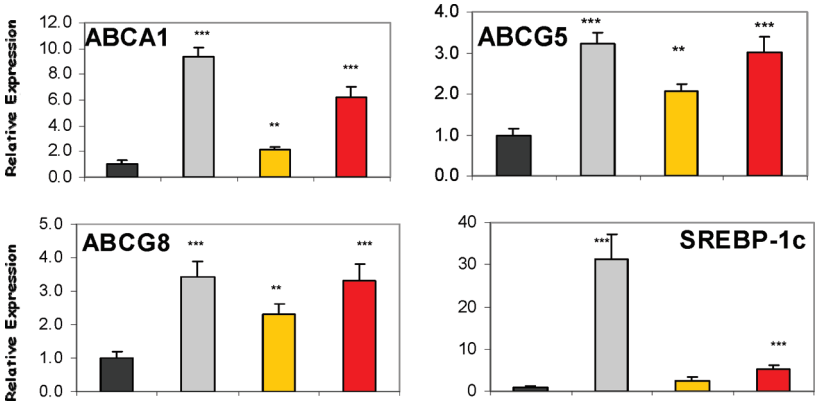

Figure 4. Effects of **13** and **1b** on target gene relative expression in duodenum. Male LDLR−/− mice (n = 5 or 6) were fed a Western diet (black bars) or diet supplemented to deliver 10 mg/kg of **1b** (gray bars), 0.6 mg/kg of compound **13** (orange bars), and 3 mg/kg compound **13** (red bars) for eight weeks. ** $p < 0.01$; *** $p < 0.001$.

3-Methyl-2-[3′-(methylsulfonyl)biphenyl-4-yl]-5-(trifluoromethyl)-quinoxaline (13). Step 1: A mixture of 2-nitro-3-(trifluoromethyl)aniline (2.6 g, 12.6 mmol), ethanol (20 mL), and 10% Pd/C (1.0 g) was pressurized with 25 psi H_2 for 1.5 h. The catalyst was removed by filtering through a short pad of celite. The filtrate (3-trifluoro-benzene-1,2-diamine solution) was mixed with 1-(4-methoxyphenyl)propane-1,2-dione (2.5 g, 14.0 mmol). The mixture was stirred at room temperature for 1 h, and the solvent was removed. The residue was purified by flash chromatography eluted with EtOAc/hexane to give 2-(4-methoxyphenyl)-3-methyl-5-(trifluoromethyl)quinoxaline (**8a**) as a pale-yellow solid (1.4 g, 35% for two steps). ^{1}H NMR (DMSO-d_6): δ 8.34 (d, J = 7.5 Hz, 1H), 8.21 (d, J = 7.1 Hz, 1H), 7.91 (t, J = 7.7 Hz, 1H), 7.77 (d, J = 8.7 Hz, 2H), 7.12 (d, J = 8.7 Hz, 2H), 3.86 (s, 3H), 2.79 (s, 3H). MS (ES) m/z 319.1.

The regio-isomer 3-(4-methoxyphenyl)-2-methyl-5-(trifluoromethyl)quinoxaline (**9a**) was also isolated in 50% yield (2 g) from the reaction mixture. ^{1}H NMR (DMSO-d_6): δ 8.31 (d, J = 7.9, 1H), 8.19 (d, J = 7.3 Hz, 1H), 7.81 (t, J = 8.0 Hz, 1H), 7.80 (d, J = 6.8 Hz, 2H), 7.14 (d, J = 6.8 Hz, 2H), 3.86 (s, 3H), 2.82 (s, 3H). MS (ES) m/z 319.1.

The regio-chemistry for **9a** was assigned based on ^{1}H−^{15}N-gHMBC NMR experiment, and the details are included in the Supporting Information.

Step 2: A mixture of **8a** (1.4 g, 4.39 mmol) and HBr (48% in water, 20 mL) in 20 mL of acetic acid was heated to 90 °C overnight. Seven mL of HBr (45%) in acetic acid was added, and the reaction mixture was heated to reflux for 5 h. The reaction mixture was poured into ice, extracted with EtOAc. The organic was concentrated and purified by flash chromatography eluted with EtOAc/hexane to give 4-[3-methyl-5-(trifluoromethyl)-quinoxalin-2-yl]phenol (**10a**) (1.20 g, 90%) as a gummy solid. ^{1}H NMR (DMSO-d_6): δ 9.86 (s, 1H), 8.28 (d, J = 7.5 Hz, 1H), 8.14 (d, J = 7.3 Hz, 1H), 7.85 (t, J = 7.7 Hz, 1H), 7.62 (d, J = 8.7 Hz, 2H), 6.88 (d, J = 8.7 Hz, 2H), 2.74 (s, 3H). MS (ESI) m/z 305.1. HRMS: calcd for $C_{16}H_{11}F_3N_2O + H^+$, 305.08962; found (ESI, $[M + H]^+$), 305.0894.

Step 3: A mixture of **10a** (1.20 g, 3.93 mmol), anhydrous THF (40 mL), and *N*-phenylbis(trifluoromethanesulfonamide) (2.11 g, 5.93 mmol) was cooled to 0 °C upon which potassium *tert*-butoxide (0.62, 5.53 mmol) was added. The resulting mixture was stirred at 0 °C for 1 h. Another portion of *N*-phenylbis-(trifluoromethanesulfonamide) (2.11 g, 5.93 mmol) and potassium *tert*-butoxide (0.62, 5.53 mmol) was added. After one more hour, the reaction was quenched with water, partitioned between water and EtOAc, and the organic was dried over $MgSO_4$. The residue was subjected to flash silica gel chromatography (hexane:EtOAc) to afford 4-[3-methyl-5-(trifluoromethyl)quinoxalin-2-yl]phenyl trifluoromethanesulfonate (**11a**) (1.2 g, 65%) as a colored solid. ^{1}H NMR ($CDCl_3$): δ 8.29 (d, J = 8.3 Hz, 1H), 8.11 (d, J = 7.0 Hz, 1H), 7.80 (d, J = 8.2 Hz, 2H), 7.48 (d, J = 8.2 Hz, 2H), 7.26 (s, 1H), 2.85 (s, 3H). MS (ES) m/z 436.9.

Step 4: A mixture of **11a** (1.2 g, 2.75 mmol), 3-methylsulfonylphenyl boronic acid (2.4 g, 12 mmol), K_3PO_4 (5.0 g, 23.6 mmol), and $Pd(PPh_3)_4$ (0.5 g, 0.43 mmol) in 40 mL of dioxane was heated to 80 °C for 1 h. The reaction mixture was poured into water and extracted with EtOAc. The organic was concentrated and purified by flash chromatography eluted with EtOAc/hexane to give **13** (0.59 g, 48%) as a white solid. ^{1}H NMR (DMSO-d_6): δ 8.40 (d, J = 8.9 Hz, 1H), 8.29−8.26 (m, 2H), 8.19 (d, J = 7.8 Hz, 1H), 8.00−7.93 (m, 6H), 7.81 (t, J = 7.8 Hz, 1H), 3.34 (s, 3H), 2.83 (s, 3H). MS (ES) m/z 443.0. HRMS: calcd for $C_{23}H_{17}F_3N_2O_2S + H^+$, 443.10356; found (ESI, $[M + H]^+$), 443.1040.

3-Methyl-2-[4′-(methylsulfonyl)biphenyl-4-yl]-5-(trifluoromethyl)-quinoxaline (14). Prepared according to the procedure of compound **13** (step 4) from **11a** and 4-methylsulfonylphenylboronic acid in 39% yield; pale-yellow solid. ^{1}H NMR ($CDCl_3$): δ 8.31 (d, J = 8.3 Hz, 1H), 8.10−8.06 (m, 3H), 7.76−7.87 (m, 7H), 3.13 (s, 3H), 2.90 (s, 3H). MS (ES) m/z 443.0. HRMS: calcd for $C_{23}H_{17}F_3N_2O_2S + H^+$, 443.10356; found (ESI, $[M + H]^+$), 443.1039.

3-Methyl-2-[2′-(methylsulfonyl)biphenyl-4-yl]-5-(trifluoromethyl)-quinoxaline (15). Prepared according to the procedure of compound **13** (step 4) from **11a** and 2-methylsulfonylphenylboronic acid in 63% yield; white solid. ^{1}H NMR (DMSO-d_6): δ 8.41 (d, J = 7.8 Hz, 1H), 8.26 (d, J = 7.2 Hz, 1H), 8.14 (d, J = 8.0 Hz, 1H), 7.96 (t, J = 8.0 Hz, 1H), 7.89 (d, J = 8.3 Hz, 2H), 7.82 (t, J = 7.4 Hz, 1H), 7.74 (t, J = 7.4 Hz, 1H), 7.61 (d, J = 8.3 Hz, 2H), 7.51 (d, J = 7.8 Hz, 1H), 3.31 (s, 3H), 2.94 (s, 3H). HRMS: calcd for $C_{23}H_{17}F_3N_2O_2S + H^+$, 443.10356; found (ESI, $[M + H]^+$), 443.1043. HRMS: calcd for $C_{23}H_{17}F_3N_2O_2S + Na^+$, 465.08550; found (ESI, $[M + Na]^+$), 465.0855.

3-Methyl-2-[3′-(methylsulfonyl)biphenyl-3-yl]-5-(trifluoromethyl)quinoxaline (16). Step 1: 2-(3-methoxyphenyl)-3-methyl-5-(trifluoromethyl)quinoxaline (**8b**) was prepared according to the procedure of **13** (step 1) from 3-trifluoromethyl-benzene-1,2-diamine and 1-(3-methoxyphenyl)propane-1,2-dione in 38%; red powder. ^{1}H NMR (DMSO-d_6): δ 9.86 (s, 1H), 8.28 (d, J = 7.5 Hz, 1H), 8.14 (d, J = 7.3 Hz, 1H), 7.85 (t, J = 7.7 Hz, 1H), 7.62 (d, J = 8.7 Hz, 2H), 6.88 (d, J = 8.7 Hz, 2H), 2.74 (s, 3H). MS (ES) m/z 319.1.

The regio-isomer 3-(3-methoxyphenyl)-2-methyl-5-(trifluoromethyl)quinoxaline (**9b**) was also isolated in 24% yield; red powder. ^{1}H NMR (DMSO-d_6): δ 8.29 (d, J = 8.4, 1H), 8.17 (d, J = 7.2 Hz, 1H), 7.90 (t, J = 8.0 Hz, 1H), 7.45 (t, J = 8.0 Hz, 1H), 7.31−7.28 (m, 2H), 7.11−7.08 (m, 1H), 3.79 (s, 3H), 2.73 (s, 3H). MS (ES) m/z 319.1.

The regio-chemistry for **8b** and **9b** was confirmed based on **10b** and **27** as shown in the Supporting Information.

Step 2: 3-[3-methyl-5-(trifluoromethyl)quinoxalin-2-yl]phenol (**10b**) was prepared from **8b** followed the procedure of **13** (step 2). ^{1}H NMR (DMSO-d_6): δ 9.70 (s, 1H), 8.36 (d, J = 7.7, 1H), 8.24 (d, J = 7.1 Hz, 1H), 7.92 (t, J = 7.9 Hz, 1H), 7.35 (t, J = 7.9 Hz, 1H), 7.20−7.12 (m, 2H), 6.95−6.92 (m, 1H), 2.75 (s, 3H). MS (ES) m/z 304.7. HRMS: calcd for $C_{16}H_{11}F_3N_2O + H^+$, 305.08962; found (ESI, $[M + H]^+$), 305.0899.

Step 3: **16** was prepared from **10b** and 3-methylsulfonylphenylboronic acid following the procedure of **13** (step 3 and step 4) in 70% yield; white solid. ^{1}H NMR (DMSO-d_6): δ 8.33 (d, J = 8.5 Hz, 1H), 8.29−8.28 (m, 1H), 8.18 (d, J = 7.3 Hz, 1H), 8.11−7.70 (m, 8H), 3.20 (s, 3H), 2.85 (s, 3H). MS (ES) m/z 443.0. HRMS: calcd for $C_{23}H_{17}F_3N_2O_2S + H^+$, 443.10356; found (ESI, $[M + H^+]$), 443.1037.

3-Methyl-2-[4′-(methylsulfonyl)biphenyl-3-yl]-5-(trifluoromethyl)quinoxaline (17). Prepared according to the procedure of compound **13** (step3 and step 4) from **10b** and 4-methylsulfonylphenylboronic acid in 35% yield; white solid. ^{1}H NMR (MeOH-d_4): δ 8.27 (d, J = 7.8 Hz, 1H), 8.12 (d, J = 6.9 Hz, 1H), 8.03−7.76 (m, 8H), 7.68 (t, J = 7.7 Hz, 1H), 3.12 (s, 3H), 2.81 (s, 3H). HRMS: calcd for $C_{23}H_{17}F_3N_2O_2S + H^+$, 443.10356; found (ESI, $[M + H]^+$), 443.1038.

2-[3′-(Ethylsulfonyl)biphenyl-4-yl]-3-methyl-5-(trifluoromethyl)-quinoxaline (18). Prepared according to the procedure of compound **13** (step 4) from **11a** and 3-ethylsulfonylphenylboronic acid in 75% yield; white solid. ^{1}H NMR (DMSO-d_6): δ 8.40 (d, J = 8.0 Hz, 1H), 8.26 (d, J = 7.5 Hz, 1H), 8.23 (br s, 1H), 8.02−7.93 (m, 6H), 7.82 (d, J=7.8 Hz, 1H), 4.43 (q, J = 7.3 Hz, 2H), 2.82 (s, 3H), 1.18 (t, J=7.3 Hz, 3H). MS (ESI) m/z 457.2. HRMS: calcd for $C_{24}H_{19}F_3N_2O_2S + H^+$, 457.11921; found (ESI, $[M + H]^+$), 457.1199. HRMS: calcd for $C_{24}H_{19}F_3N_2O_2S + Na^+$, 479.10115; found (ESI, $[M + Na]^+$), 479.1012.

***N*-Methyl-4′-[3-methyl-5-(trifluoromethyl)quinoxalin-2-yl]biphenyl-3-sulfonamide (19).** Step 1, 2-(4-chlorophenyl)-3-methyl-5-(trifluoromethyl)quinoxaline (**8c**) and 3-(4-chlorophenyl)-2-methyl-5-(trifluoromethyl)quinoxaline (**9c**): **8c** was prepared from 1-(4-chlorophenyl)propane-1,2-dione and 3-(trifluoromethyl)benzene-1,2-diamine according to the procedure of **13** (step 1) in 36% yield; white solid. ^{1}H NMR ($CDCl_3$): δ 8.28 (d, J = 8.3 Hz, 1H), 8.10 (d, J = 7.3 Hz, 1H), 7.77 (d, J = 7.8 Hz, 1H), 7.63 (d, J = 8.3 Hz, 2H), 7.54 (d, J = 8.3 Hz, 2H), 2.84 (s, 3H). HRMS: calcd for $C_{16}H_{10}ClF_3N_2 + H^+$, 323.05573; found (ESI, $[M + H]^+$), 323.0557.

The regio-isomer (**9c**) was also isolated in 32% yield; white solid. ^{1}H NMR ($CDCl_3$): δ 8.23 (d, J = 8.3 Hz, 1H), 8.07 (d, J = 7.3 Hz, 1H), 7.77 (d, J = 7.8 Hz, 1H), 7.75 (d, J = 8.3 Hz, 2H), 7.52 (d, J = 8.3 Hz, 2H), 2.86 (s, 3H). HRMS: calcd for $C_{16}H_{10}ClF_3N_2 + H^+$, 323.05573; found (ESI, $[M + H]^+$), 323.0557.

The regio-chemistry of **8c** and **9c** was assigned as shown in the Supporting Information.

Step 2: A mixture of **8c** (0.06 g, 0.26 mmol), 3-(*N*-methylsulfamoyl)phenylboronic acid (0.15 g, 0.70 mmol), K_3PO_4 (0.3 g, 1.4 mmol), dicyclohexyl(2′,6′-dimethoxybiphenyl-2-yl)phosphine (0.04 g, 0.1 mmol), and $Pd(OAc)_2$ (0.02 g, 0.09 mmol) in 5 mL of 1-butanol was heated to 80 °C for 1 h. The reaction mixture was concentrated and purified by flash chromatography eluted with EtOAc/hexane to give **19** (0.036 g, 42%) as a white solid. ^{1}H NMR (DMSO-d_6): δ 8.40 (d, J = 8.3 Hz, 1H), 8.26 (d, J = 7.4 Hz, 1H), 8.14 (br s, 1H), 8.12 (d, J = 7.7 Hz, 1H),8.08−7.92 (m, 5H), 7.82 (d, J = 6.5 Hz, 1H), 7.78 (t, J= 7.7 Hz, 1H), 7.54 (s, 1H), 3.31 (s, 3H), 2.83 (s, 3H). MS (ESI) m/z 458.1;. HRMS: calcd for $C_{23}H_{18}F_3N_3O_2S + H^+$, 458.11446; found (ESI, $[M + H]^+$), 458.1145. HRMS: calcd for $C_{23}H_{18}F_3N_3O_2S + Na^+$, 480.09640; found (ESI, $[M + Na]^+$), 480.0965.

***N*-Methyl-4′-[3-methyl-5-(trifluoromethyl)quinoxalin-2-yl]biphenyl-3-carboxamide (20).** Prepared according to the procedure of compound **19** (step 2) from **8c** and 3-(methylcarbamoyl)phenylboronic acid in 48% yield; white solid. ^{1}H NMR (DMSO-d_6): δ 8.62−8.58 (m, 1H), 8.40 (d, J = 7.5 Hz, 1H), 8.27−8.23 (m, 2H), 7.97−7.89 (m, 7H), 7.61 (t, J = 7.7 Hz, 1H), 3.23 (s, 3H), 2.84 (s, 3H). MS (ESI) m/z 422.2. HRMS: calcd for $C_{24}H_{18}F_3N_3O + H^+$, 422.14747; found (ESI, $[M + H]^+$), 422.1475. HRMS: calcd for $C_{24}H_{18}F_3N_3O + Na^+$, 444.12941; found (ESI, $[M + Na]^+$), 444.1294.

3-Ethyl-2-[3′-(methylsulfonyl)biphenyl-4-yl]-5-(trifluoromethyl)-quinoxaline (21). Step 1: 4-[3-ethyl-8-(trifluoromethyl)quinoxalin-2-yl]phenol (**10d**) was prepared according to the procedure of **13** (step 1 and 2) from 2-nitro-3-(trifluoromethyl)-aniline and 1-(4-methoxyphenyl)butane-1,2-dione in 7% yield for the two steps; crystal solid. ^{1}H NMR ($CDCl_3$): δ 8.28 (d, J = 8.7 Hz, 1H), 8.05 (d, J = 6.8 Hz, 1H), 7.76 (d, J = 8.3 Hz, 1H), 7.68 (d, J = 8.3 Hz, 2H), 7.00 (d, J = 8.3 Hz, 2H), 3.21 (q, J = 7.3 Hz, 2H), 1.37 (t, J = 7.3 Hz, 3H). HRMS: calcd for $C_{17}H_{13}F_3N_2O + H^+$, 319.10527; found (ESI, $[M + H]^+$), 319.1053.

The regio-isomer of **10d** (compound **28**) was also isolated in 14% yield; pale-yellow solid. ^{1}H NMR ($CDCl_3$): δ 8.31 (d, J = 8.3 Hz, 1H), 8.06 (d, J = 7.2 Hz, 1H), 7.75 (d, J = 7.7 Hz, 1H), 7.53 (d, J = 8.3 Hz, 2H), 6.93 (d, J = 8.3 Hz, 2H), 3.12 (q, J = 7.3 Hz, 2H), 1.38 (t, J = 7.3 Hz, 3H); HRMS: calcd for $C_{17}H_{13}F_3N_2O + H^+$, 319.10527; found (ESI, $[M + H]^+$), 319.1053.

The regio-chemistry for **10d** and **28** was assigned as shown in the Supporting Information.

Step 2: **21** was prepared according to the procedure of **13** (step 3 and step 4) from **10d** and 3-methylsulfonylphenyl boronic acid in 33% yield; off-white solid. ^{1}H NMR (DMSO-d_6): δ 8.40 (d, J = 8.3 Hz, 1H), 8.28−8.26 (m, 2H), 8.17 (d, J = 8.0 Hz, 1H), 8.02−7.85 (m, 6H), 7.81 (t, J = 7.8 Hz, 1H), 3.39 (s, 3H), 3.12 (q, J = 7.8 Hz, 2H), 1.31 (t, J = 7.8 Hz, 3H). MS (ESI) m/z 457.1. HRMS: calcd for $C_{24}H_{19}F_3N_2O_2S + H^+$, 457.11921; found (ESI, $[M + H]^+$), 457.1191.

2-[3′-(Methylsulfonyl)biphenyl-4-yl]-5-(trifluoromethyl)quinoxaline (22). Step 1: 2-(4-methoxyphenyl)-5-(trifluoromethyl)-quinoxaline (**8e**) was prepared according to the procedure of **13** (step 1) from 2-nitro-3-(trifluoromethyl)aniline and 2-(4-methoxyphenyl)-2-oxoacetaldehyde as a solid in 6% yield. ^{1}H NMR (DMSO-d_6): δ 9.72 (s, 1H), 8.40−8.35 (m, 3H), 8.21 (d, J=7.1 Hz, 1H), 7.98 (t, J=7.3 Hz, 1H), 7.18 (d, J=8.8 Hz, 2H), 3.88 (s, 3H). MS (ES) m/z 304.9. The regio-isomer 2-(4-methoxyphenyl)-8-(trifluoromethyl)quinoxaline (**9e**) was also isolated as a pale-yellow solid in 59% yield. ^{1}H NMR (DMSO-d_6): δ 9.72 (s, 1H), 8.41−8.36 (m, 3H), 8.26 (d, J = 7.2 Hz, 1H), 7.92 (t, J = 7.9 Hz, 1H), 7.20 (d, J = 7.9 Hz, 2H), 3.88 (s, 3H). MS (ES) m/z 304.9;

The regio-chemistry for **8e** and **9e** was assigned as shown in the Supporting Information.

Step 2: **22** was prepared according to the procedure of **13** (step 2, step 3, and step 4) from **8e** and 3-methylsulfonylphenyl boronic acid in 9% yield; off-white solid. ^{1}H NMR ($CDCl_3$): δ 9.54 (s, 1H), 8.39−8.35 (m, 3H), 8.26 (s, 1H), 8.12 (d, J = 7.0 Hz, 1H), 8.00−7.96 (m, 2H), 7.89−7.85 (m, 3H), 7.72 (t, J = 7.8 Hz, 1H), 3.14 (s, 3H). HRMS: calcd for $C_{22}H_{15}F_3N_2O_2S + H^+$, 429.08791; found (ESI, $[M + H]^+$), 429.0883. HRMS: calcd for $C_{22}H_{15}F_3N_2O_2S + Na^+$, 451.06985; found (ESI, $[M + Na]^+$), 451.0698.

5-Chloro-3-methyl-2-[3′-(methylsulfonyl)biphenyl-4-yl]quinoxaline (23). A mixture of 1-(4-chlorophenyl)propane-1,2-dione (3.0 g, 16.5 mmol), 3-methylsulfonylphenyl boronic acid (6.6 g, 33 mmol), KF (2.87 g, 49.5 mmol), dicyclohexyl(biphenyl-2-yl)phosphine (1.16 g, 3.3 mmol), and $Pd(OAc)_2$ (0.37 g, 1.65 mmol) in 100 mL of THF was stirred at room temperature for a day. The reaction mixture was concentrated and purified by flash chromatography eluted with EtOAc/hexane to give 1-(3′-(methylsulfonyl)biphenyl-4-yl)propane-1,2-dione as a yellow solid (0.3 g, ∼90% pure). The yellow solid (0.15 g, 0.5 mmol) was dissolved in ethanol (5 mL), and 3-chloro-benzene-1,2-diamine (0.07 g, 0.5 mmol) was added. After being stirred at room temperature overnight, the reaction mixture was concentrated and purified by flash chromatography eluted with EtOAc/hexane to give **23** (0.025 g, 12%) as a slight-colored solid. ^{1}H NMR (DMSO-d_6): δ 8.28 (s, 1H), 8.17 (d, J = 7.9 Hz,

1H), 8.10 (d, J = 8.3 Hz, 1H), 8.04−7.90 (m, 6H), 7.82 (d, J = 7.0 Hz, 1H), 7.80 (d, J = 7.7 Hz, 1H), 3.34 (s, 3H), 2.83 (s, 3H). MS (ESI) m/z 409.1. HRMS: calcd for $C_{22}H_{17}ClN_2O_2S + H^+$, 409.07720; found (ESI, $[M + H]^+$), 409.0772. HRMS: calcd for $C_{22}H_{17}ClN_2O_2S + Na^+$, 431.05914; found (ESI, $[M + Na]^+$), 431.0591.

The regio-isomer 5-chloro-2-methyl-3-[3′-(methylsulfonyl)-biphenyl-4-yl]quinoxaline (**29**) was also isolated as a slight-colored solid (30 mg, 14% yield). ^{1}H NMR (DMSO-d_6): δ 8.29−8.28 (m, 1H), 8.16 (d, J = 6.8 Hz, 1H), 8.07 (d, J = 8.4 Hz, 1H), 8.05−7.70 (m, 8H), 3.34 (s, 3H), 2.82 (s, 3H). MS (ESI) m/z 409.1. MS (ESI) m/z 447.1. HRMS: calcd for $C_{22}H_{17}ClN_2O_2S + H^+$, 409.07720; found (ESI, $[M + H]^+$), 409.0775. HRMS: calcd for $C_{22}H_{17}ClN_2O_2S + Na^+$, 431.05914; found (ESI, $[M + Na]^+$), 431.0587.

3-Methyl-2-[3′-(methylsulfonyl)biphenyl-4-yl]quinoxaline-5-carbonitrile (24). Step 1: 2-(4-chlorophenyl)-3-methylquinoxaline-5-carbonitrile (**8f**) was prepared according to the procedure of **18** (step 1) from 1-(4-chlorophenyl)propane-1,2-dione and 3-cyano-benzene-1,2-diamine in 20% yield; white solid. ^{1}H NMR ($CDCl_3$): δ 8.33 (d, J = 8.4 Hz, 1H), 8.15 (d, J = 7.2 Hz, 1H), 7.78 (d, J = 8.4 Hz, 1H), 7.65 (d, J = 8.6 Hz, 2H), 7.54 (d, J = 8.6 Hz, 2H), 2.88 (s, 3H). HRMS: calcd for $C_{16}H_{10}ClN_3 + H^+$, 280.06360; found (ESI, $[M + H]^+$) 280.0636.

The regio-isomer 3-(4-chlorophenyl)-2-methylquinoxaline-5-carbonitrile (**9f**) was also isolated in 20% yield; white solid. ^{1}H NMR ($CDCl_3$): δ 8.28 (d, J = 8.4 Hz, 1H), 8.13 (d, J = 7.5 Hz, 1H), 7.80 (d, J = 7.3 Hz, 1H), 7.77 (d, J = 8.7 Hz, 2H), 7.55 (d, J = 8.7 Hz, 2H), 2.87 (s, 3H). HRMS: calcd for $C_{16}H_{10}ClN_3 + H^+$, 280.06360; found (ESI, $[M + H]^+$), 280.0636.

The regio-chemistry for **8f** and **9f** was assigned as shown in the Supporting Information.

Step 2: **24** was prepared according to the procedure of **18** (step 2) from **8f** and 3-methylsulfonylphenyl boronic acid in 29% yield; white solid. ^{1}H NMR (DMSO-d_6): δ 8.46−8.44 (m, 2H), 8.29 (br s, 1H), 8.17 (d, J = 7.8 Hz, 1H), 8.01−7.94 (m, 6H), 7.81 (t, J = 7.8 Hz, 1H), 3.34 (s, 3H), 2.86 (s, 3H). HRMS: calcd for $C_{23}H_{17}N_3O_2S + H^+$, 400.11142; found (ESI, $[M + H]^+$, 400.1115.

5-Methoxy-3-methyl-2-[3′-(methylsulfonyl)biphenyl-4-yl]quinoxaline (25). Step 1: 2-(4-chlorophenyl)-5-methoxy-3-methylquinoxaline (**8g**) was prepared according to the procedure of **18** (step 1) from 1-(4-chlorophenyl)propane-1,2-dione and 3-methoxy-benzene-1,2-diamine in 21% yield; white solid. ^{1}H NMR (DMSO-d_6): δ 7.79 (d, J = 8.1 Hz, 2H), 7.71 (t, J = 8.3 Hz, 1H), 7.64−7.60 (m, 3H), 7.27 (d, J = 7.8 Hz, 1H), 4.02 (s, 3H), 2.70 (s, 3H). MS (ESI) m/z 285.1. HRMS: calcd for $C_{16}H_{13}ClN_2O + H^+$, 285.07892; found (ESI, $[M + H]^+$), 285.0794. HRMS: calcd for $C_{16}H_{13}ClN_2O + Na^+$, 307.06086; found (ESI, $[M + Na]^+$), 307.0609.

The regio-isomer 3-(4-chlorophenyl)-5-methoxy-2-methylquinoxaline (**9g**) was also isolated in 19% yield; white solid. ^{1}H NMR (DMSO-d_6): δ 7.77 (d, J = 8.2 Hz, 2H), 7.75 (t, J = 8.2 Hz, 1H), 7.63 (d, J = 7.8 Hz, 2H), 7.60 (d, J = 8.5 Hz, 1H), 7.25 (d, J = 7.9 Hz, 1H), 4.00 (s, 3H), 2.80 (s, 3H). MS (ESI) m/z 285.1. HRMS: calcd for $C_{16}H_{13}ClN_2O + H^+$, 285.07892; found (ESI, $[M + H]^+$), 285.0789. HRMS: calcd for $C_{16}H_{13}ClN_2O + Na^+$, 307.06086; found (ESI, $[M + Na]^+$), 307.0609.

The regio-chemistry for **8g** and **9g** was assigned as shown in the Supporting Information.

Step 2: **25** was prepared according to the procedure of **18** (step 2) from **8g** and 3-methylsulfonylphenyl boronic acid in 88% yield; white solid. ^{1}H NMR (DMSO-d_6): δ 8.28 (s, 1H), 8.16 (d, J = 7.8 Hz, 1H), 8.00−7.90 (m, 5H), 7.81 (t, J = 7.8 Hz, 1H), 7.72 (t, J = 8.0 Hz, 1H), 7.63 (d, J = 8.4 Hz, 1H), 7.28 (d, J = 7.9 Hz, 1H), 4.02 (s, 3H), 3.33 (s, 3H), 2.77 (s, 3H). MS (ESI) m/z 405.2. HRMS: calcd for $C_{23}H_{20}N_2O_3S + H^+$, 405.12674; found (ESI, $[M + H]^+$), 405.1267. HRMS: calcd for $C_{23}H_{20}N_2O_3S + Na^+$, 427.10868; found (ESI, $[M + Na]^+$), 427.1087.

In Vitro Assays. LXRα and LXRβ binding assays (Table 1), Gal4 transactivation assays in huh-7 liver cells (Table 2 and 3), ABCA1 gene regulation in THP-1 cells (Table 2), C-efflux, and NHR cross reactivity screens were performed as described previously.[8] Gal4 transactivation assays in kidney HEK-293 (Table 3) were performed as described in ref 23.

TG Accumulation in HepG2 Cells. Results for compounds in Table 2 were obtained using methods previously described.[24]

Peptide Recruitment Assay. Results for compounds in Figure 3 were obtained using methods previously described.[11b]

LDLR −/− Mouse Inhibition of Lesion Progression Model. Eight-week old male LDLR−/− mice were fed atherogenic diet or diet supplemented to deliver compounds **1b** or **13** for 8 weeks. Aortas were obtained and analyzed using methods previously described.[8]

Acknowledgment. We thank the Wyeth Discovery Analytic Chemistry Department for the analytical data and Anita Halpern and Dawn Savio for biological assay data. We gratefully acknowledge Drs. Ron Magolda (deceased on June 1, 2008), Magid Abou-Gharbia, Tarek Mansour, Steve Gardell, and George Vlasuk for their support of this work.

Supporting Information Available: ^{1}H−^{15}N-gHMBC NMR experiments, HPLC purity for the final compounds, Figure A (Effects of **13** and **1b** on Target Gene Relative Expression in macrophages), and Figure B (Low Density array survey of gene activation in liver indicates little regulation by compound **1b** and **13**). This material is available free of charge via the Internet at http://pubs.acs.org.

References

(1) Fievet, C.; Staels, B. Liver X receptor modulators: Effects on lipid metabolism and potential use in the treatment of atherosclerosis. *Biochem. Pharmacol.* **2009**, *77*, 1316–1327.

(2) Zhang, Y; Chan, J.; Cummins, C. Liver X receptors as therapeutic targets for managing cholesterol: implications for inflammatory conditions. *Clin. Lipidol.* **2009**, *4*, 29–40.

(3) Gabbi, C; Warner, M.; Gustafsson, J. Minireview: liver X receptor b: emerging roles in physiology and diseases. *J. Mol. Endocrinol.* **2009**, *23*, 129–136.

(4) (a) Bennett, D. J.; Carswell, E. L.; Cooke, A. J.; Edwards, A. S.; Nimz, O. Design, structure−activity relationships and X-ray co-crystallography of non-steroidal LXR agonists. *Curr. Med. Chem.* **2008**, *15*, 195–209. (b) Goodwin, B. J.; Zuercher, W. J.; Collins, J. L. Recent advances in Liver X Receptor biology and chemistry. *Curr. Top. Med. Chem.* **2008**, *8*, 781–791.

(5) Schultz, J. R.; Tu, H.; Luk, A.; Repa, J. J.; Medina, J. C.; Li, L. P.; Schwendner, S.; Wang, S.; Thoolen, M.; Mangelsdorf, D. J.; Lustig, K. D.; Shan, B. Role of LXRs in control of lipogenesis. *Genes Dev.* **2000**, *14* (22), 2831–2838.

(6) Collins, J. L.; Fivush, A. M.; Watson, M. A.; Galardi, C. M.; Lewis, M. C.; Moore, L. B.; Parks, D. J.; Wilson, J. G.; Tippin, T. K.; Binz, J. G.; Plunket, K. D.; Morgan, D. G.; Beaudet, E. J.; Whitney, K. D.; Kliewer, S. A.; Willson, T. M. Identification of a Nonsteroidal Liver X Receptor Agonist through Parallel Array Synthesis of Tertiary Amines. *J. Med. Chem.* **2002**, *45*, 1963–1966.

(7) Joseph, S. B.; McKilligin, E.; Pei, L.; Watson, M. A.; Collins, A.; Laffitte, B. A.; Chen, M.; Noh, G.; Goodman, J.; Hagger, G. N.; Tran, J.; Tippin, T. K.; Wang, X.; Lusis, A. J.; Hsueh, W. A.; Law, R. E.; Collins, J. L.; Willson, T. M.; Tontonoz, P. Synthetic LXR ligand inhibits the development of atherosclerosis in mice. *Proc. Natl. Acad. Sci. U.S.A* **2002**, *99*, 7604–7609.

(8) Hu, B.; Collini, M.; Unwalla, R.; Miller, C.; Singhaus, R.; Quinet, E.; Savio, D.; Halpern, A.; Basso, M.; Keith, J.; Clerin, V.; Chen, L.; Resmini, C.; Liu, Q.-Y.; Feingold, I.; Huselton, C.; Azam, F.; Farnegardh, M.; Enroth, C.; Bonn, T.; Goos-Nilsson, A.; Wilhelmsson, A.; Nambi, P.; Wrobel, J. Discovery of Phenyl Acetic Acid Substituted Quinolines as Novel Liver X Receptor Agonists for the Treatment of Atherosclerosis. *J. Med. Chem.* **2006**, *49*, 6151–6154.

(9) Hu, B.; Jetter, J.; Kaufman, D.; Singhaus, R.; Bernotas, R.; Unwalla, R.; Quinet, E.; Savio, D.; Halpern, A.; Basso, M.; Keith, J.; Clerin, V.; Chen, L.; Liu, Q.-Y.; Feingold, I.; Huselton, C.;

Azam, F.; Goos-Nilsson, A.; Wilhelmsson, A.; Nambi, P.; Wrobel, J. Further Modifications on Phenyl Acetic Acid Based Quinolines as Liver X Receptor Modulators. *Bioorg. Med. Chem.* **2007**, *15*, 3321–3333.

(10) Wrobel, J.; Steffan, R.; Bowen, M.; Magolda, R.; Matelan, E.; Unwalla, R.; Basso, M.; Clerin, V.; Gardell, S.; Nambi, P.; Quinet, E.; Reminick, J. I.; Vlasuk, G.; Wang, S.; Feingold, I.; Huselton, C.; Bonn, T.; Farnegardh, M.; Hansson, T.; Nilsson, A.; Wilhelmsson, A.; Zamaratski, E.; Evans, M. Indazole-based LXR Modulators with Maintained Atherosclerotic Lesion Reduction Activity but Diminished Stimulation of Hepatic Triglyceride Synthesis. *J. Med. Chem.* **2008**, *51*, 7161–7168.

(11) (a) Katz, A.; Udata, C.; Ott, E.; Hickey, L.; Burczynski, M.; Burghart, P.; Vesterqvist, O.; Meng, X. Safety, pharmacokinetics, and pharmacodynamics of single doses of LXR-623, a novel liver X-receptor agonist, in healthy participants. *J. Clin. Pharmacol.* **2009**, *49*, 643–649. (b) Quinet, E. M.; Basso, M. D.; Halpern, A. R.; Yates, D. W.; Steffan, R. J.; Clerin, V.; Resmini, C.; Keith, J. C.; Berrodin, T. J.; Feingold, I.; Zhong, W.; Hartman, H. B.; Evans, M. J.; Gardell, S. J.; DiBlasio-Smith, E.; Mounts, W. M.; LaVallie, E. R.; Wrobel, J.; Nambi, P.; Vlasuk, G. P. LXR ligand lowers LDL cholesterol in primates, is lipid neutral in hamster, and reduces atherosclerosis in mouse. *J. Lip. Res.* **2009**, *50*, 2358–2370.

(12) (a) Bradley, M. N.; Hong, C.; Chen, M.; Joseph, S. B.; Wilpitz, D. C.; Wang, X.; Lusis, A. J.; Collins, A.; Hseuh, W. A.; Collins, J. L.; Tangirala, R. K.; Tontonoz, P. Ligand activation of LXRb reverses atherosclerosis and cellular cholesterol overload in mice lacking LXRa and apoE. *J. Clin. Invest.* **2007**, *117*, 2337–2346. (b) By using LXRa−/− mice and LXRb−/− mice the role of LXRa and LXRb has been extensively studied, for a review on the subtype influence on TG synthesis see: ref 3: (c) Lund, E. G.; Peterson, L. B.; Adams, A. D.; Lam, M. N.; Burton, C. A.; Chin, J.; Guo, Q.; Huang, S.; Latham, M.; Lopez, J. C.; Maenke, J. G.; Milot, D. P.; Mitnaul, L. J.; Rex-Rabe, S. E.; Rosa, R. L.; Tian, J. Y.; Wright, S. D.; Sparrow, C. P. Different roles of liver X receptor α and β in lipid metabolism: Effects of an α-selective and a dual agonist in mice deficient in each subtype. *Biochem. Pharmacol.* **2006**, *71*, 453–463. (d) Quinet, E.; Savio, D.; Halpern, A.; Chen, L.; Schuster, G. U.; Gustafsson, J.; Basso, M.; Nambi, P. Liver X Receptor (LXR)-Regulation in LXR-Deficient Mice: Implications for Therapeutic Targeting. *Mol. Pharmacol.* **2006**, *70*, 1340–1349.

(13) (a) Faernegardh, M; Bonn, T.; Sun, S.; Ljunggren, J.; Ahola, H.; Wilhelmsson, A.; Gustafsson, J.-A.; Carlquist, M. The Three-dimensional Structure of the Liver X Receptor b Reveals a Flexible Ligand-Binding Pocket That Can Accommodate Fundamentally Different Ligands. *J. Biol. Chem.* **2003**, *278*, 38821–38828. (b) Williams, S.; Bledsoe, R. K.; Collins, J. L.; Boggs, S.; Lambert, M. H.; Miller, A. B.; Moore, J.; McKee, D. D.; Moore, L.; Nichols, J.; Parks, D.; Watson, M.; Wisely, B.; Willson, T. M. X-ray Crystal Structure of the Liver X Receptor b Ligand Binding Domain: Regulation by a Histidine−Tryptophan Switch. *J. Biol. Chem.* **2003**, *278*, 27138–27143.

(14) Molteni, V.; Li, X.; Nabakka, J.; Liang, F.; Wityak, J.; Koder, A.; Vargas, L.; Romeo, R.; Mitro, N.; Mak, P. A.; Seidel, H. M.; Haslam, J. A.; Chow, D.; Tuntland, T.; Spalding, T. A.; Brock, A.; Bradley, M.; Castrillo, A.; Tontonoz, P.; Saez, E. *N*-Acylthiadiazolines, a New Class of Liver X Receptor Agonists with Selectivity for LXRb. *J. Med. Chem.* **2007**, *50*, 4255–4259.

(15) (a) Kratzer, A.; Buchebner, M.; Pfeifer, T.; Becker, T.; Uray, G.; Miyazaki, M.; Miyazaki-Anzai, S.; Ebner, B.; Chandak, P.; Kadam, R.; Calayir, E.; Rathke, N.; Ahammer, H.; Radovic, B.; Trauner, M.; Hoefler, G.; Kompella, U.; Fauler, G.; Levi, M.; Levak-Frank, S.; Kostner, G.; Kratky, D. Synthetic LXR agonist attenuates plaque formation in apoE−/− mice without inducing liver steatosis and hypertriglyceridemia. *J. Lip. Res.* **2009**, *50*, 312–326. (b) Quinet, E.; Savio, D.; Halpern, A.; Chen, L.; Miller, C.; Nambi, P. Gene-selective modulation by a synthetic oxysterol ligand of the liver X receptor. *J. Lip. Res.* **2004**, *45*, 1929–1942.

(16) Hu, B.; Unwalla, R.; Collini, M.; Quinet, E.; Feingold, I.; Goos-Nilsson, A.; Wihelmsson, A.; Nambi, P.; Wrobel, J. Discovery and SAR of cinnolines/quinolines as liver X receptor (LXR) agonists with binding selectivity for LXRb. *Bioorg. Med. Chem. Lett.* **2009**, *19*, 3519–3527.

(17) Travins, J.; Bernotas, R.; Kaufman, D.; Quinet, E.; Nambi, P.; Feingold, I.; Huselton, C.; Wilhelmsson, A.; Goos-Nilsson, A.; Wrobel, J. 1-(3-Aryloxyaryl)benzimidazole sulfones are liver X receptor agonists. *Bioorg. Med. Chem. Lett.* **2010**, *20*, 526–530.

(18) Travins, J.; Bernotas, R.; Unwalla, R.; Evans, M.; Quinet, E.; Basso, M.; Nambi, P.; Feingold, I.; Wilhelmsson, A.; Goos-Nilsson, A.; Wrobel, J. Quinazoline biarylether sulfones as LXR ligands with improved LXRb selectivity and lower triglyceride potential, Abstracts of Papers, 238th ACS National Meeting, Washington, DC, August 16−20, 2009, MEDI-390.

(19) Bernotas, R.; Singhaus, R.; Kaufman, D.; Ullrich, J.; Fletcher, H.; Quinet, E.; Nambi, P.; Unwalla, R.; Wilhelmsson, A.; Goos-Nilsson, A.; Farnegardh, M.; Wrobel, J. Biarylether amide quinolines as liver X receptor agonists. *Bioorg. Med. Chem. Lett.* **2009**, *19*, 1663–1670.

(20) *GLIDE, Version 4.5*; Schrodinger, LLC: Portland, OR, 2007.

(21) Hu, B.; Bernotas, R.; Unwalla, R.; Collini, M.; Quinet, E.; Feingold, I.; Goos-Nilsson, A.; Wilhelmsson, A.; Nambi, P.; Evans, M.; Wrobel, J. Quinoline-3-carboxamide Containing Sulfones as Liver X Receptor (LXR) Agonists with Binding Selectivity for LXRb and Low Blood Brain Penetration. *Bioorg. Med. Chem. Lett.* **2010**, *20*, 632–635.

(22) Both compound **13** and **16** had good mouse liver microsome stability ($T_{1/2}$ > 30 min) but low solubility in the Gal4 biological buffer (∼0.1 mM). No significant difference was found for the uptake of these two compounds in the huh-7 cells (0.89 mmol in cells for **13** vs 0.63 mmol for **26** after 1 h treatment; 3.79 mmol in cells for **13** vs 1.35 mmol for **26** after 7 h treatment).

(23) Pawar, A.; Xu, J.; Jerks, E.; Mangelsdorf, D.; Jump, J. Fatty Acid Regulation of Liver X Receptors (LXR) and Peroxisome Proliferator-activated Receptor α (PPARa) in HEK293 Cells. *J. Biol. Chem.* **2002**, *277*, 39243–39250.

(24) Hu, B.; Quinet, E.; Unwalla, R.; Collini, M.; Jetter, J.; Dooley, R.; Andrake, D.; Nogle, L.; Savio, D.; Halpern, A.; Goos-Nilsson, A.; Wilhelmsson, A.; Nambi, P.; Wrobel, J. Carboxylic Acid Based Quinolines As Liver X Receptor Modulators That Have LXRb Receptor Binding Selectivity. *Bioorg. Med. Chem. Lett.* **2008**, *18*, 54–59.